See discussions, stats, and author profiles for this publication at: https://www.researchgate.net/publication/48879496

Trends in EPR g-tensors and hyperfine coupling constants of the isomer pairs HCO/COH, HCS/CSH, HSiO/SiOH and HSiS/SiSH

ARTICLE in CHEMICAL PHYSICS · JANUARY 2004	
Impact Factor: 1.65 · DOI: 10.1016/j.chemphys.2003.09.031 · Source: OAI	
CITATIONS	READS
9	21

1 AUTHOR:

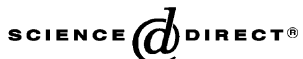


F. Grein
University of New Brunswick

245 PUBLICATIONS 3,135 CITATIONS

SEE PROFILE





Chemical Physics 296 (2004) 71-78

Chemical Physics

www.elsevier.com/locate/chemphys

Trends in EPR g-tensors and hyperfine coupling constants of the isomer pairs HCO/COH, HCS/CSH, HSiO/SiOH and HSiS/SiSH

Friedrich Grein *

Department of Chemistry, University of New Brunswick, P.O. Box 45222, Fredericton, NB, Canada E3B 6E2

Received 5 August 2003; accepted 25 September 2003

Abstract

For the isomer pairs HCO/COH, HCS/CSH, HSiO/SiOH and HSiS/SiSH (HXY/XYH), electron-spin g-tensors and hyperfine coupling constants are calculated. Comparison is made with experimental results for HCO and HSiO, obtained from EPR studies, and with g-shifts ($\Delta g = g - g_c$) calculated via Curl's equation from spin-rotation coupling constants for HCO, CSH, HSiO and HSiS. For HCO, the large component of the g-shift, Δg_{yy} (y is along XY), is calculated to be -7885 ppm, compared with an EPR value of -7500 ppm, and a Curl's value of -7975 ppm. For HSiO, the corresponding numbers are (in ppm) -8685, -5100 and -7375. Hyperfine coupling constants (HFCCs) are in good agreement with available experimental data. Interesting trends have been established and explained. The y-component of the g-shift is smaller for HXY than for XYH, except for HCS. The isotropic HFCCs have the opposite ordering. They are larger for HXY than for XYH, except for HCS. For the heavy atoms (13 C, 29 Si, 17 O, 33 S), A_{iso} (X) is always larger for HXY than for XYH, and A_{dip} (X) always smaller for HXY than for XYH, indicating that the atom bonded to hydrogen receives s-spin density at the expense of p-spin density.

1. Introduction

According to theoretical studies, HCO [1], HCS [2] and HSiS [3] (HXY) are more stable than their XYH isomers, by about 40 kcal/mol for the first two, and by about 4 kcal/mol for the last one. On the other hand, HSiO is predicted to be less stable than SiOH, by about 9 kcal/mol [4,5].

Microwave spectra have been obtained for HCO [6], HCS [7–9] and HSiS [10], as well as for the less stable radicals CSH [9,11] and HSiO [12]. Despite its much higher energy, the discovery of CSH is aided by its dipole moment being larger than that of HCS (CSH is more strongly bent than HCS), and by the fact that it lies energetically lower than its dissociation products H+CS (contrary to COH).

The major goal of this work is the evaluation of electron-spin *g*-tensors and hyperfine coupling constants

(HFCCs) for HCO, HCS, HSiO and HSiS and their isomers, all having ²A' ground states. For HCO [13–15] and HSiO [16] experimental EPR values are available (there is also some EPR evidence for SiOH [16]). In addition, microwave studies on HCO, CSH, HSiO and HSiS, cited above, recorded hyperfine coupling constants as well as spin–rotation coupling constants, from which via Curl's equation [17] *g*-values can be estimated. In a laser magnetic resonance (LMR) study performed on HCO [18], *g*-factors and proton HFCCs were obtained.

Isotropic proton hyperfine coupling constants have been calculated for HCO, HCS, HSiO and HSiS by Chen and Huang [19], and found to be in good agreement with experimental values known from microwave studies. Such is also the case for the anisotropic proton HFCC of HCS. A detailed study on the hyperfine structure of the X²A' and A²A'' states of HCO, including vibronic effects, has been performed by Staikova et al. [20]. Theoretical results for HCO have also been given by Nakano et al. [21] and Morihashi et al. [22]. Rani and Ray [23] calculated HFCCs for HSiO and SiOH, whereas Petraco et al. [24] and Webster [25], reported results for HCS.

^{*}Tel.: +5064534776; fax: +5064534981. *E-mail address:* fritz@unb.ca (F. Grein).

Due to the importance of these radicals in interstellar molecular clouds, as well as in combustion processes, and the fact that two of the less stable isomers have been observed, the present study is intended to help in the eventual identification of the yet unobserved isomers. As will be seen, EPR parameters for the two isomers of each compound differ drastically, and EPR studies are therefore well suited for their discovery. In addition, using the present results, systematic trends have been established for g-values and hyperfine coupling constants, leading to a better understanding of these (often unpredictable) magnetic properties.

2. Methods

For each radical, geometry optimizations were performed using the MP2/6-311++G** method and the Gaussian 98 programs [26]. While the geometries of some radicals are known from experimental, and others from theoretical studies, it was found best to use a consistent set of geometries obtained by the same method. In any case, the deviations from experimental values are small.

The g-tensor components are obtained from multireference configuration-interaction (MRCI) wavefunctions, using second-order perturbation theory with explicit sum-over-states expansions. The method is described in earlier references [27]. The programs used here employ the MRCI method of Grimme and Waletzke [28], which is based on the Turbomole package [29] for efficient integral and SCF calculations. The spin-orbit integrals are calculated by the Hess-Marian mean-field method [30], as implemented by Schimmelpfennig [31] and adapted for the Grimme MRCI package by Kleinschmidt et al. [32] (see [33] for recent applications of these methods). The TZVPP valence triple-zeta basis set with polarization functions by Schäfer et al. [34] was employed in the g-tensor calculations. For each irreducible representation, nine roots were used in the sumover-states expansions. In all cases, the last few roots made vanishing contributions to the sum, indicating that the calculated values had sufficiently converged. The electronic charge centroid (ECC) is always taken as gauge origin. First-order terms for the g-tensor components are usually quite small, with g-shifts ($g-g_{\rm e}$) in the order of 100 ppm [27], and are not included here. Since the molecules have $C_{\rm s}$ symmetry, the in-plane components (x and y) mix, and matrix diagonalization is required.

Previous experience with these methods [27,33,35,36] has shown that the large components of Δg usually lie within 10% of the experimental value, but for the small components, in the order of 100–1000 ppm, such good percentage agreement is not possible.

3. Results and discussion

In Table 1, the MP2/6-311++G** optimized geometries, as used in further calculations, and the corresponding energies, are given. In agreement with literature values, HXY is usually more stable than XYH, except for HSiO, which is calculated to be 9.1 kcal/mol less stable than SiOH. The isomerization energies are large for HCO (45.4 kcal/mol) and HCS (39.5 kcal/mol), but small for HSiO (9.1 kcal/mol) and HSiS (4.4 kcal/mol), as pointed out in Section 1.

3.1. EPR g-tensors

In Table 2, the Δg values ($\Delta g = g - g_{\rm e}$) are displayed. For HCO and HSiO, experimental values from EPR (and LMR) studies are included in Table 2. For HCO, CSH, HSiO and HSiS, Table 2 also gives Δg values obtained via Curl's relation ($\Delta g = -\epsilon/2A$, where A is the respective rotational constant) from the spin–rotation coupling constants $\epsilon_{\rm aa}$, $\epsilon_{\rm bb}$, $\epsilon_{\rm cc}$ listed in the microwave papers.

For all radicals, the largest component in magnitude is Δg_w , which is always negative. The y-coordinate lies

Table 1 Optimized geometries ($\mathring{\mathbf{A}}$, °), corresponding energies (a.u.) and energy differences ΔE (kcal/mol), for HXY and XYH radicals in their X²A' ground state, as obtained from MP2/6-311++G** calculations

Radical	r_{XY}	$r_{\mathrm{XH}},r_{\mathrm{YH}}$	α	Energy	ΔE
HCO	1.1829	1.1218	124.3	-113.599291	0.0
СОН	1.2805	0.9774	111.4	-113.526976	45.4
HCS	1.5099	1.0930	133.6	-436.155207	0.0
CSH	1.6478	1.3568	101.8	-436.092327	39.5
HSiO	1.5417	1.5092	122.3	-364.637827	9.1
SiOH	1.6704	0.9620	119.4	-364.652314	0.0
HSiS	1.9544	1.5001	119.4	-687.226280	0.0
SiSH	2.1204	1.3401	99.7	-687.219218	4.4

Table 2 Calculated Δg components (ppm) for HXY and XYH radicals, with X = C, Si and Y = O, S, using the TZVPP basis set

Radical	Δg_{xx}	Δg_{yy}	Δg_{zz}
HCO	-85	-7885	2175
EPR [15]	0	-7500	1400
Microwave [6]	-210	-7975	2460
LMR [18]	-200	-7970	2460
СОН	-55	-12,605	470
HCS	-285	-40,755	4995
CSH	35	-6955	1430
Microwave [11]	-895	-5530	270
HSiO	-120	-8685	3560
EPR [16]	700	-5100	700
Microwave [12]	-1590	-7375	3755
SiOH	120	-94,805	-1190
HSiS	-860	-19,780	11,725
Microwave [10]	-6300	-15,550	15,380
SiSH	-1890	-43,410	4740

along the XY bond direction. This is followed by Δg_{zz} , always positive except for SiOH. The z-coordinate corresponds to the out-of-plane direction. The in-plane Δg_{xx} component is the smallest in magnitude.

For HCO experimental values are well reproduced by our calculations. The difference between the EPR matrix and the microwave/LMR values relate mainly to matrix effects. It is seen that our calculated numbers are closer to the gas-phase microwave values, indicating a fair degree of accuracy in our results. Theoretical *g*-tensor results (in ppm) for HCO obtained by other groups cover a range from -180 to -270 ppm for Δg_{xx} , from -6860 to -12300 ppm for Δg_{yy} and from 2070 to 3300 ppm for Δg_{zz} [37].

In the microwave paper on HCS [7], only an effective ϵ_{ii} -value is given, which relates to Δg_{xx} and Δg_{zz} , and is therefore not useful for a comparison. For CSH, however, all three components of the spin–rotation coupling constant have been reported, from which we derived the Δg values of Table 2. For Δg_{yy} , reasonable agreement is seen, whereas the smaller components are not so well reproduced.

An interesting situation is noted for HSiO/SiOH. Van Zee et al. [16] observed the EPR spectrum of HSiO in a Ne matrix and remarked on its similarity to that of HCO. The authors were aware of the fact that theoretical calculations placed the SiOH isomer at lower energy, and attributed the formation of HSiO instead of SiOH to their particular method of preparation. For HSiO, the agreement between calculated and experimental EPR values is reasonable, but not as good as we are accustomed to. The experimental Δg_{yy} differs by about 40% from the calculated value (-5100 vs. -8685 ppm). However, as for HCO, such deviations may be due mainly to matrix effects, as indicated by the microwave data for Δg_{yy} and Δg_{zz} lying quite close to our

calculated numbers. A large disagreement is still seen for Δg_{xx} , which is calculated to be -120 ppm, but has a microwave value of -1590 ppm (and an EPR value of 700 ppm). In any case, the observed isomer is clearly HSiO and not SiOH, since for the latter Δg_{yy} is about 10 times larger in magnitude.

Microwave values for HSiS show that our calculated value for Δg_{yy} is too large in magnitude by 27%, whereas Δg_{zz} is too small by a similar percentage. Also, Δg_{xx} is too small in magnitude.

It is noticed that $|\Delta g_{yy}|$ is usually much larger for the XYH than for the corresponding HXY isomer, the exception being HCS/CSH. In order to explain this observation, Table 3 lists the values of the SO_y and L_y matrix elements as well as ΔE for the coupling of $1^2A''$ with the X^2A' ground state. (In second-order perturbation theory, each term of the sum-over-states expansion for Δg is of the form $(SO \times L)/\Delta E$. For the Δg_{yy} component, ΔE refers to the vertical excitation energy of the $^2A''$ states, given in Table 4, of which the first one makes the largest contribution to Δg_{yy} .) For all radicals, the L_y s are similar, ranging from -0.78 to -0.99 a.u. For each isomer pair, the SO_y values are also similar, except for HCS/CSH, where SO_y of HCS is about four times that

Table 3 Contribution from the $1^2A''$ state to $\Delta g'_{yy}$ (before matrix diagonalization)

Radical	SO_y	L_y	ΔE	$\Delta g_{yy}^{'}$
НСО	35.1	-0.92	2.16	-7650
COH	23.1	-0.97	0.93	$-12,\!270$
HCS	75.5	-0.93	0.94	-38,000
CSH	18.4	-0.91	1.44	-5940
HSiO	40.3	-0.80	2.51	-6550
SiOH	63.4	-0.99	0.34	-94,250
HSiS	80.1	-0.78	2.01	-15,690
SiSH	63.6	-0.95	0.71	-43,300

 SO_y , spin-orbit matrix element (cm⁻¹); L_y , angular momentum matrix element (a.u.) and ΔE , excitation energy of $1^2A''$ (eV). TZVPP basis set.

Table 4 Vertical excitation energies (eV) for low-lying $^2A'$ and $^2A''$ valence states of HXY and XYH radicals with X^2A' ground state, using the TZVPP basis set

	$2^{2}A^{'}$	$3^2A'$	$4^2A'$	$1^2A^{''}$	$2^2A^{\prime\prime}$	$3^2A''$
HCO	6.07	6.82	7.47	2.16	7.00	7.67
COH	4.32	5.68	7.59	0.93	6.14	7.55
HCS	4.30	5.44	5.90	0.94	4.86	5.05
CSH	3.23	4.77	5.19	1.44	4.14	4.50
HSiO	3.26	4.33	5.15	2.51	3.38	5.06
SiOH	3.09	4.72	5.56	0.34	4.95	6.26
HSiS	2.39	3.85	4.40	2.01	2.58	3.98
SiSH	3.50	4.20	4.46	0.71	4.04	4.40

of CSH. Significant differences, however, are seen for ΔE . For each pair, there is a low and a high ΔE , differing by a factor of 7 in the case of HSiO/SiOH. As a consequence, the isomer with the lower ΔE has the higher Δg_{yy} . The smaller ΔE (and larger Δg_{yy}) is usually associated with the XYH isomer, except for HCS/CSH. This ΔE abnormality for the latter pair combined with the low SO_y for CSH causes $|\Delta g_{yy}|$ of CSH to be much smaller than that of HCS.

Why is ΔE of XYH usually smaller than that of HXY? One may visualize the process of H⁺ approaching XY⁻. The XY⁻ anion is an 11 valence-electron system, with a ${}^{2}\Pi$ GS, having π^{*} as the singly occupied MO (SOMO). The approaching H⁺ splits $X^2\Pi$ of XY^- into ${}^{2}A'$ and ${}^{2}A''$, or the π^{*} SOMO into a' and a''. For CO⁻, SiO⁻ and SiS⁻, the π^* -SOMO is mainly localized on C or Si (contrary to electronegativity (EN) values, which apply to the π MO). Therefore, if H⁺ attaches to C or Si, the in-plane a becomes stabilized (the a SOMO is σ -like), whereas approach from the other side (O or S) gives little stabilization to a', and the a'-SOMO remains π -like. In other words, the a -SOMO of HCO, HSiO and HSiS is σ -like, whereas it is π -like for COH, SiOH and SiSH. This qualitative picture is confirmed by the orbital energies of the a'-SOMO and a"-LUMO (lowest unoccupied MO), given in Table 5. (MO plots for HCO/COH are given in the paper by Staikova et al. [20], and for HSiO/SiOH by Bruna and Grein [4].) For the σ -radicals HCO, HSiO and HSiS, ϵ_{SOMO} is *lower* than for the corresponding XYH isomer. On the other hand, for HCS ϵ_{SOMO} is higher than for the corresponding CSH isomer, reflecting the π^* localization in CS⁻ on S, not on C (again, opposite to EN values). Therefore, HCS is a π radical, and CSH a σ-radical, in contrast to the other systems, where the H–C or H–Si bonded isomer is of σ character. Since ϵ_{LUMO} is virtually the same for each pair of isomers (Table 5), $\Delta \epsilon$ (and ΔE) is larger for HCO, HSiO and HSiS than for the respective other isomer, and smaller for HCS than for CSH. A smaller ΔE leads to the larger Δg . The magnetic coupling, as reflected in the L matrix element, is always large (around 1 a.u.)

Table 5 Orbital energies ϵ (a.u.) for the a'-SOMO and a"-LUMO of HXY and XYH isomers, from MP2/6-311++G** calculations

	$\epsilon_{ m SOMO}$	$\epsilon_{ m LUMO}$	$\Delta\epsilon$
HCO	-0.396	0.072	0.468
COH	-0.363	0.079	0.442
HCS	-0.327	0.038	0.365
CSH	-0.393	0.049	0.442
HSiO	-0.389	0.009	0.398
SiOH	-0.271	0.019	0.290
HSiS	-0.350	-0.003	0.347
SiSH	-0.296	0.006	0.302

between two states that result from the splitting of a Π state, corresponding in this case to the X^2A' and $1^2A''$ states of HXY/XYH.

All Δg_{yy} are negative, since the dominant excited state in the SOS expansion, $1^2A''$, results from a SOMO \rightarrow LUMO excitation, which in general leads to a negative Δg [17].

The out-of-plane component, Δg_{zz} , is of medium size, always lying in magnitude between Δg_{xx} and Δg_{yy} . It is positive except for SiOH due to the dominant ²A' excited state being of DOMO (doubly occupied MO) to SOMO type (for HCO, 2²A' results from a 6a' to 7a' excitation, where 7a' is the SOMO). For SiOH, however, this state is of SOMO-virtual MO type. While the individual SO and L matrix elements are of similar magnitude as those obtained for Δg_{xx} and Δg_{yy} , the ²A' excitation energies are usually much higher than the ²A" ones, starting at around 6 eV for HCO (Table 4). The Δg_{zz} component lacks the low-energy/high-L excited state, and is therefore not as large in magnitude as Δg_{yy} . The Δg_{xx} component, on the other hand, while profiting from the low excitation energies of the ²A" states, has positive and negative contributions from a number of states, and is therefore small in magnitude, and not traceable to coupling with any particular excited state.

Habara et al. [7], in their millimeter-wave study of HCS, predict ϵ_{aa} (and $|\Delta g_{yy}|$) of HCS to be much larger than that of HCO, based on the larger bond angle of HCS, implying a weaker Renner-Teller interaction than in HCO. From this they conclude that $1^2A''$ should be lower in HCS than in HCO, and consequently ϵ_{aa} (HCS) higher than that of HCO. Although they could not obtain ϵ_{aa} , their prediction is confirmed in the present study.

In several cases, the excitation energy of 1²A" has been predicted from ϵ_{aa} (corresponding to Δg_{yy}) by applying the Curl equation. It is common to set the angular momentum matrix element equal to -1 a.u., and to use atomic values for the spin-orbit matrix element. For CSH, Habara and Yamamoto [11] obtain an excitation energy of 1.29 eV (10,400 cm⁻¹), compared with the calculated value of 1.44 eV (Table 4). Izuha et al. [12] estimate this excitation energy for HSiO to be about 5 eV (40,000 cm⁻¹), compared with the calculated value of 2.51 eV. A large discrepancy between the assumed spinorbit matrix element (148.9 cm⁻¹, the value of Si) and the calculated value of 40.3 cm⁻¹, as well as differences in L_y , are responsible for such deviation. For HSiS, Brown et al. [10] estimate the excitation energy to be 2.37 eV (19,100 cm⁻¹), using for SO_v again the Si value of 148.9 cm⁻¹. The calculated energy is 2.01 eV, and SO_v is 80.1 cm^{-1} .

It is obvious that the isomer with the lower-energy SOMO does not have to be the more stable one, since the overall bonding in the HXY systems is not confined to the SOMO. While HCO and HSiS have the lower-

energy SOMO and are more stable than their corresponding isomer, such is not the case for CSH and HSiO, which are less stable than their isomers despite having the more stable SOMO.

3.2. Proton hyperfine coupling constants

For the optimized geometries, given in Table 1, isotropic and anisotropic proton HFCCs were calculated using the B3LYP/6-311++G** method. The results are given in Table 6. Spin densities (SD) on the protons are also included.

For $A_{iso}(H)$, the agreement with experimental values, obtained from microwave studies on HCO, HCS, HSiO and HSiS, as well as EPR studies on HSiO, is good, with deviations of about 12% for HCO and HSiO, 9% for HSiS and 2% for HCS. In all cases, the calculated $A_{iso}(H)$ s are smaller than experimental values. Theoretical results obtained by Chen and Huang [19], also given in Table 6, show somewhat better agreement with experimental values, which was found to be due to small differences in geometry. Using the experimental geometry for HCO, an A_{iso} of 347.8 MHz is obtained. With the Chen and Huang geometry, it is 353.8 MHz. Changing the basis set, for example to 6-311G(3df,3pd), brought no overall improvement in the A_{iso} s. Therefore, for the unknown systems, underestimation errors up to about 10% are expected.

Theoretical results for $A_{\rm iso}({\rm H})$ obtained by other groups are as follows (in MHz): for HCO, 335/353, depending on geometry [20], 339 [21], 315–355, depending on method [22]; for HCS 121.1 [24], 114.1 [25]; for HSiO 418 [23] and for SiOH 53 [23].

The striking feature of Table 6 is seen in the relation between the $A_{\rm iso}$ s for the two isomers of each pair. For the σ -radicals HCO, HSiO and HSiS, $A_{\rm iso}({\rm H})$ of HXY is larger than that of XYH, whereas $A_{\rm iso}({\rm H})$ of the π -radical HCS is smaller than that of CSH. Exactly the reverse ordering was seen for $|\Delta g_{yy}|$. There, $|\Delta g_{yy}({\rm HXY})|$ was smaller than $|\Delta g_{yy}({\rm XYH})|$ for HCO, HSiO and HSiS, and larger for HCS. It is obvious that a correlation exists between $A_{\rm iso}({\rm H})$ and Δg_{yy} .

The trends for the Δg_{yy} component of the *g*-tensor could be explained by the SOMO of the σ -radical being lower in energy than the SOMO of the corresponding π -radical, due to the better bonding to hydrogen in the case of the σ -SOMO. Equivalently, the SOMO of the σ -radical should have a larger spin density on H than the SOMO of the π -radical. Such is clearly seen in the Mulliken SD(H) values given in Table 6. For HCO, HSiO and HSiS, the higher SD(H) resides on the HXY isomer, whereas for the HCS system it resides on CSH. This hydrogen spin density is mainly of s-type, and therefore directly related to $A_{\rm iso}({\rm H})$. The fact that σ -radicals have larger $A_{\rm iso}({\rm H})$ values is well documented in the literature [13,16,17].

Using for the hydrogen atom $A_{\rm iso}({\rm H}) = 1420~{\rm MHz}$ [17], the percent s-spin density has been calculated for each radical, and is also given in Table 6. For the σ -radicals, such percentages range from 19% for CSH to 30% for HSiO, whereas for the π -radicals values from 4% for SiOH to 14% for COH have been obtained. These percent s-spin densities are somewhat larger, but roughly proportional to the Mulliken values SD(H) discussed above.

The amount of p-spin density on H, related to the $A_{\rm dip}$ values, is more difficult to estimate. According to

Table 6	
Proton spin densities (SD) and hyperfine coupling constants (MHz) from B3LVP/6-311++G** calculations	

	SD(H)	$A_{ m iso}$	s-SD (%)	$T_{ m aa}{}^{ m a}$	$T_{ m bb}{}^{ m a}$	$T_{ m cc}{}^{ m a}$
НСО	0.159	343.1	25	23.2	-7.4	-15.8
Expt. [6]		388.9				
Expt. [15]		354		25	-8	-17
Theor. [19]		356.9				
COH	0.069	191.9	14	17.8	-7.8	-10
HCS	0.046	125.3	9	27.4	-6.3	-21.1
Expt. [9]		127.1		15.1		
Theor. [19]		129.1		30.6	-7.0	-23.5
CSH	0.133	249.5	19	8	-3.5	-4.5
Expt. [9]		290.5		5.4	-0.6	
HSiO	0.236	397.1	30	5.6	-1.0	-4.6
Expt. [12]		451.3				
Expt. [16]		450				
Theor. [19]		417.7				
SiOH	0.016	51.3	4	10.9	-3.7	-7.2
HSiS	0.173	304.9	22	5.4	-0.9	-4.5
Expt. [10]		335.7				
Theor. [19]		315.3				
SiSH	0.053	109.6	8	5.2	-1.8	-3.32

 $^{^{}a}$ T_{aa} is mainly the in-plane XH, YH direction; T_{bb} in-plane perpendicular to XH, YH; T_{cc} the out-of-plane direction.

System Atom HXY XYH $A_{\rm iso}$ $A_{\rm iso}$ $A_{\rm dip}$ $A_{\rm dip}$ ^{13}C HCO/COH 377.6a 87.8 57.6 178.4 17**O** -27.7^{b} -109.5-53.2-22.913 C HCS/CSH 267.6° 96.8 49.1^d 157.1e ^{33}S 10.8 76.7 38.3 10.5 ²⁹Si HSiO/SiOH -591.1^f -100.3-4.5 -204.1^{g} ^{17}O -13.1-85.2-21-17.5 ^{29}Si HSiS/SiSH -544.7-98.71.9 -206.4 ^{33}S 3.2 75.6 21.6 4.9

Table 7
Hyperfine coupling constants (MHz) for the heavy atoms, from B3LYP/6-311++G** calculations

the calculated values, for HCO/COH the p-character is proportional to the s-character, but for the HCS and HSiO pairs, the isomer with the larger $A_{\rm iso}$ has much smaller $A_{\rm dip}$ values. For HSiS/SiSH, $A_{\rm dip}$ s are about the same, although $A_{\rm iso}$ is much smaller for SiSH. Such details are related to the particular structure of the SOMO. For example, while the SOMO of HCS shows some p-character on H, that of CSH has no p-lobe on the proton.

3.3. Hyperfine coupling constants for the heavy atoms

In Table 7, $A_{\rm iso}$ and $A_{\rm dip}$ values are given for ¹³C, ²⁹Si, ¹⁷O and ³³S, calculated by B3LYP/6-311++G**. For $A_{\rm dip}$, the component $T_{\rm cc}$ has been chosen, which is the largest in magnitude of the three $T_{\rm S}$. In most cases, $T_{\rm aa} \approx T_{\rm bb} \approx -1/2T_{\rm cc}$. $T_{\rm cc}$ is usually oriented along the inplane direction perpendicular to XY, except for S in CSH and SiSH, where it is rotated more towards XY.

EPR results for $A_{\rm iso}(^{13}{\rm C})$ of HCO are 377.5 MHz [14] and 365 MHz [15]. Habara et al. [9] give $A_{\rm iso}(^{13}{\rm C})$ values of 287.9 MHz for HCS, and 47.9 MHz for CSH. An experimental value for $A_{\rm iso}(^{29}{\rm Si})$ of HSiO in a Ne matrix [16] is ± 665 MHz, compared with our result of -591 MHz.

Both for $A_{\rm iso}$ and $A_{\rm dip}$ values, trends can be easily recognized. The heavy atom bonded to H has always the higher $|A_{\rm iso}|$ and the lower $|A_{\rm dip}|$. For the HXY/XYH pair, X of HXY, and Y of XYH, have the larger $|A_{\rm iso}|$, and the smaller $|A_{\rm dip}|$. For HCO/COH, $A_{\rm iso}(^{13}{\rm C})$ of HCO is about six times larger than that of COH, whereas $A_{\rm dip}(^{13}{\rm C})$ of HCO is only about one half the value for COH. On the other hand, for COH $|A_{\rm iso}(^{17}{\rm O})|$ is larger and $|A_{\rm dip}(^{17}{\rm O})|$ smaller than for HCO. This rule even applies to the HCS/CSH pair, for which the proton $A_{\rm iso}$ values behaved opposite to those for the other systems, due to HCS being a π -

radical, whereas the other HXY compounds are σ -radicals.

The explanation for the trends in the HFCCs is quite straightforward. The atom next to H benefits from the spin density of H (larger $A_{\rm iso}$), at the expense of p-density (smaller $A_{\rm dip}$). One might expect that for HCS, the transfer of s-density from H to C is not as good as for the other HXY systems, but such evidence is not seen in the ratio of the $A_{\rm iso}$ values for C or S. On the other hand, $A_{\rm iso}({\rm Si})$ in HSiO and HSiS is 100 to 300 times larger than in the corresponding SiOH and SiSH isomers.

For all HXY systems, $|A_{\rm dip}({\rm Y})|$ is much larger than $|A_{\rm iso}({\rm Y})|$, due to Y having larger p-density. Correspondingly, for XYH, $|A_{\rm dip}({\rm X})|$ is much larger than $|A_{\rm iso}({\rm X})|$.

Using the respective atomic $A_{\rm iso}$ and $A_{\rm dip}$ values as given by Weltner [17], it can be seen that the total (s + p) spin density on XY is 90–95% for the π -radicals SiOH, SiSH and HCS, and between 70% and 85% for the other radicals.

4. Summary and conclusion

For the isomer pairs HXY/XYH, with X=C, Si and Y=O, S, g-tensors and hyperfine coupling constants were calculated. For the g-tensors, sum-overstate expansions (second-order perturbation theory) based on MRCI wavefunctions were employed with a valence triple-zeta and polarization basis set. For HFCCs, B3LYP/6-311++G** calculations were performed.

Agreement with experimental values obtained from EPR studies on HCO and HSiO, and from microwave studies on HCO, HCS, CSH, HSiO and HSiS is good.

^a Ref. [14], exptl., 377.5 MHz; Ref. [15], exptl., 365 MHz; Ref. [20], theor., 385, 398 MHz.

^b Ref. [20], theor., -41.1 MHz.

^c Ref. [9], exptl., 287.9 MHz.

^d Ref. [9], exptl., 47.9 MHz.

^eRef. [9], exptl., 142.6 MHz.

^fRef. [16], exptl., 665 MHz.

^g Ref. [16], exptl., 166 MHz.

The largest component (in magnitude) of the g-shift, $|\Delta g_{yy}|$, is much larger for XYH than for HXY, the exception being the HCS/CSH pair, where $|\Delta g_{vv}|$ for HCS is about six times larger than for CSH. This can be easily explained. In second-order perturbation theory, the y-component of the g-shift results mainly from the coupling of the ${}^{2}A'$ ground state with the ${}^{12}A''$ excited state. The g-shift is given by the formula $(SO \times L)/\Delta E$. The spin-orbit (SO) and angular momentum (L) matrix elements are essentially the same for the two isomers, but the difference lies in the energy separation ΔE . The orbital energy of the a SOMO is lower for the σ -isomers HCO, HSiO, HSiS and CSH than for the corresponding π -isomer, resulting in a higher excitation energy for the 1²A" state (the energy of the a"-LUMO is about the same for the two isomers).

Exactly the opposite trend is seen for the isotropic proton HFCCs. The σ -radicals (HCO, CSH, HSiO and HSiS) have larger, and the π -radicals (COH, HCS, SiOH and SiSH) smaller $A_{\rm iso}({\rm H})$, reflecting the fact that the SOMO of the σ -radical is stabilized by bonding to H, resulting in a higher s-spin density on H. Trends for the anisotropic proton HFCCs could not be established.

For the heavy atom, $A_{\rm iso}(X)$ is always larger for HXY than for XYH, and $A_{\rm dip}(X)$ smaller for HXY than for XYH. The heavy atom bonded to H has larger s-spin density and smaller p-spin density than the other heavy atom which is not bonded to H.

It has been shown that EPR parameters are very sensitive to the atomic sequence in the HXY/XYH isomers, with g-shifts and hyperfine coupling constants changing by factors from 2 to 10 from one isomer to the other. Due to such properties, EPR studies are ideally suited to distinguish between such isomers.

A correlation has been found for the trends in *g*-tensors with those in hyperfine coupling constants. The isomer with the large *y*-component of the *g*-tensor has the smaller proton isotropic hyperfine coupling constant.

In future studies, this type of work is to be extended to other $HXY^{(+,-)}$ radicals with 11 valence electrons, like HBO^- and HCN^- , and to corresponding systems where the hydrogen is substituted by F or Cl, like $FXY^{(\pm)}$ and $CIXY^{(\pm)}$. Many of these radicals are known from experimental studies.

Acknowledgements

Support for this work by a research grant from NSERC (Canada) is gratefully acknowledged. We thank Drs. Pablo Bruna and Scott Brownridge from this University for reading the manuscript and for making helpful suggestions, and Prof. Stefan Grimme from the

University of Muenster, and Prof. Christel Marian from the University of Duesseldorf, for making their computer programs available to us.

References

- A.V. Marenich, J.E. Boggs, J. Phys. Chem. A 107 (2003) 2343, and references therein.
- [2] C. Ochsenfeld, R.I. Kaiser, Y.T. Lee, M. Head-Gordon, J. Chem. Phys. 110 (1999) 9982.
- [3] P.J. Bruna, F. Grein, J. Phys. Chem. 96 (1992) 6617.
- [4] P.J. Bruna, F. Grein, Mol. Phys. 63 (1988) 329.
- [5] Y. Yamaguchi, Y. Xie, S.-J. Kim, H.F. Schaefer III, J. Chem. Phys. 105 (1996) 1951.
- [6] G. Blake, K.V.L.N. Sastry, F.C. De Lucia, J. Chem. Phys. 80 (1984) 95.
- [7] H. Habara, S. Yamamoto, C. Ochsenfeld, M. Head-Gordon, R.I. Kaiser, Y.T. Lee, J. Chem. Phys. 108 (1998) 8859.
- [8] H. Habara, S. Yamamoto, T. Amano, J. Chem. Phys. 116 (2002) 9232
- [9] H. Habara, S. Yamamoto, J. Mol. Spectrosc. 219 (2003) 30.
- [10] F.X. Brown, S. Yamamoto, S. Saito, J. Mol. Struct. 413–414 (1997) 537.
- [11] H. Habara, S. Yamamoto, J. Chem. Phys. 112 (2000) 10905.
- [12] M. Izuha, S. Yamamoto, S. Saito, J. Mol. Struct. 413–414 (1997)
- [13] F.J. Adrian, E.L. Cochran, V.A. Bowers, J. Chem. Phys. 36 (1962) 1661.
- [14] E.L. Cochran, F.J. Adrian, V.A. Bowers, J. Chem. Phys. 44 (1966) 4626.
- [15] R.J. Holmberg, J. Chem. Phys. 51 (1969) 3255.
- [16] R.J. Van Zee, R.F. Ferrante, W. Weltner, J. Chem. Phys. 83 (1985) 6181.
- [17] W. Weltner Jr., Magnetic Atoms and Molecules, Dover, New York, 1983.
- [18] J.M. Brown, H.E. Radford, T.J. Sears, J. Mol. Spectrosc. 148 (1991) 20.
- [19] B.-Z. Chen, M.-B. Huang, Chem. Phys. Lett. 308 (1999) 256.
- [20] M. Staikova, M. Peric, B. Engels, S.D. Peyerimhoff, J. Mol. Spectrosc. 166 (1994) 423.
- [21] T. Nakano, K. Morihashi, O. Kikuchi, Bull. Chem. Soc. Jpn. 65 (1992) 603.
- [22] K. Morihashi, Y. Shimodo, O. Kikuchi, J. Mol. Struct. (Theochem) 617 (2002) 47.
- [23] S. Rani, N.K. Ray, Indian J. Chem. A 39 (2000) 75.
- [24] N.D.K. Petraco, S.S. Wesolowski, M.L. Leininger, H.F. Schaefer III, J. Chem. Phys. 112 (2000) 6245.
- [25] B. Webster, J. Chem. Soc. Faraday Trans. 94 (1998) 1385.
- [26] M.J. Frisch, G.W. Trucks, H.B. Schlegel, G.E. Scuseria, M.A. Robb, J.R. Cheeseman, V.G. Zakrzewski, J.A. Montgomery Jr., R.E. Stratmann, J.C. Burant, S. Dapprich, J.M. Millam, A.D. Daniels, K.N. Kudin, M.C. Strain, O. Farkas, J. Tomasi, V. Barone, M. Cossi, R. Cammi, B. Mennucci, C. Pomelli, C. Adamo, S. Clifford, J. Ochterski, G.A. Petersson, P.Y. Ayala, Q. Cui, K. Morokuma, D.K. Malick, A.D. Rabuck, K. Raghavachari, J.B. Foresman, J. Cioslowski, J.V. Ortiz, B.B. Stefanov, G. Liu, A. Liashenko, P. Piskorz, I. Komaromi, R. Gomperts, R.L. Martin, D.J. Fox, T. Keith, M.A. AlLaham, C.Y. Peng, A. Nanayakkara, C. Gonzalez, M. Challacombe, P.M.W. Gill, B. Johnson, W. Chen, M.W. Wong, J.L. Andres, C. Gonzalez, M. Head-Gordon, E.S. Replogle, J.A. Pople, GAUSSIAN 98, Revision A.9, Gaussian, Inc., Pittsburgh, PA, 1998.

- [27] (a) G.H. Lushington, F. Grein, J. Chem. Phys. 106 (1995) 3292;
 (b) G.H. Lushington, P. Bündgen, F. Grein, Int. J. Quantum Chem. 55 (1995) 377;
 - (c) G.H. Lushington, F. Grein, Theor. Chim. Acta 93 (1996) 259;(d) G.H. Lushington, F. Grein, Int. J. Quantum Chem. 60 (1996) 1679.
- [28] S. Grimme, M. Waletzke, J. Chem. Phys. 111 (1999) 5645;
 S. Grimme, M. Waletzke, Phys. Chem. Chem. Phys. 2 (2000) 2075.
- [29] R. Ahlrichs, M. Bär, M. Häser, H. Horn, C. Kölmel, Chem. Phys. Lett. 162 (1989) 165.
- [30] B.A. Hess, C.M. Marian, U. Wahlgren, O. Gropen, Chem. Phys. Lett. 251 (1996) 365.

- [31] B. Schimmelpfennig, Atomic Spin-Orbit Mean-Field Integral Program, Stockholms Universitet, Sweden, 1996.
- [32] M. Kleinschmidt, J. Tatchen, C.M. Marian, J. Comput. Chem. 23 (2002) 824.
- [33] S. Brownridge, F. Grein, J. Tatchen, M. Kleinschmidt, C.M. Marian, J. Chem. Phys. 118 (2003) 9552.
- [34] A. Schäfer, C. Huber, R. Ahlrichs, J. Chem. Phys. 100 (1994) 5829.
- [35] P.J. Bruna, F. Grein, J. Mol. Struct. (Theochem) 617 (2002) 149.
- [36] P.J. Bruna, F. Grein, J. Chem. Phys. 117 (2002) 2103.
- [37] K.M. Neyman, D.I. Ganyushin, A.V. Matveev, V.A. Nasluzov, J. Phys. Chem. A 106 (2002) 5022, and references therein.